Geophysical Research Letters

RESEARCH LETTER
10.1029/2025GL119542

Structural Response of Laser-Driven Shock Compressed Albite

Sota Takagi[1], Naoko Takahashi[2], Minsu Jang[1], Huijeong Hwang[3], Jinhyuk Choi[4], Hyunseung Lee[5], Yongmoon Lee[5,6], Donghoon Seoung[7], Hiroki Kobayashi[8], Norimasa Ozaki[9,10], Tatiana Pikuz[9], Hirotaka Nakamura[9], Alexis Amouretti[9], Toshinori Yabuuchi[11,12], Kohei Miyanishi[12], and Donghoon Kim[1]

[1]Department of Earth and Environmental Sciences, Korea University, Seoul, Republic of Korea, [2]Department of Earth Science, Graduate School of Science, Tohoku University, Miyagi, Japan, [3]Department of Environment and Energy Engineering, Gwangju Institute of Science and Technology (GIST), Gwangju, Republic of Korea, [4]Pohang Light Source, PAL-II, Gyeongbuk, Republic of Korea, [5]Department of Geological Sciences, Pusan National University, Busan, Republic of Korea, [6]Institute for Future Earth, Pusan National University, Busan, Republic of Korea, [7]Department of Geological and Environmental Sciences, Chonnam National University, Gwangju, Republic of Korea, [8]Geochemical Research Center, Graduate School of Science, The University of Tokyo, Tokyo, Japan, [9]Graduate School of Engineering, Osaka University, Osaka, Japan, [10]Institute of Laser Engineering, Osaka University, Osaka, Japan, [11]Japan Synchrotron Radiation Research Institute, Hyogo, Japan, [12]RIKEN SPring-8 Center, Hyogo, Japan

Key Points:

- In situ XRD shows that the albite Hugoniot above ~30–40 GPa is dominated by amorphization rather than a hollandite-type phase
- Decomposition of albite into jadeite or Ca-ferrite-type phases is kinetically suppressed during nanosecond shock compression
- These results directly constrain short-timescale kinetics, refining interpretations of shock metamorphism in natural shocked plagioclase

Supporting Information:

Supporting Information may be found in the online version of this article.

Correspondence to:

D. Kim,
donghoonkim@korea.ac.kr

Citation:

Takagi, S., Takahashi, N., Jang, M., Hwang, H., Choi, J., Lee, H., et al. (2026). Structural response of laser-driven shock compressed albite. *Geophysical Research Letters*, *53*, e2025GL119542. https://doi.org/10.1029/2025GL119542

Received 17 SEP 2025
Accepted 2 JUN 2026

Author Contributions:

Conceptualization: Sota Takagi, Naoko Takahashi
Data curation: Sota Takagi, Naoko Takahashi, Minsu Jang, Huijeong Hwang, Jinhyuk Choi, Hyunseung Lee, Hiroki Kobayashi, Donghoon Kim
Formal analysis: Sota Takagi
Funding acquisition: Sota Takagi, Naoko Takahashi, Yongmoon Lee, Donghoon Seoung, Norimasa Ozaki, Donghoon Kim
Investigation: Sota Takagi
Methodology: Sota Takagi, Norimasa Ozaki, Tatiana Pikuz, Hirotaka Nakamura, Alexis Amouretti, Toshinori Yabuuchi, Kohei Miyanishi
Supervision: Donghoon Kim

Abstract Plagioclase records characteristic shock features that constrain meteorite impact conditions, but its phase evolution along the Hugoniot remains unresolved. We investigated shock-induced phase transition in albite using in situ X-ray diffraction during laser-driven shock at 14–66 GPa. Albite retained its crystal structure up to at least 14 GPa and underwent complete amorphization above 28 GPa, at pressures lower than those reported in shock-recovery experiments. No hollandite-type phase, jadeite, or Ca-ferrite-type $NaAlSiO_4$ was observed during shock loading, indicating that the high-pressure region of the albite Hugoniot is dominated by amorphization. Upon decompression, crystalline peaks reappeared, indicating structural recovery, which may contribute to the wide range of amorphization pressures in the recovery experiments. The absence of decomposition products indicates strong kinetic suppression under nanosecond shock durations, defining the short-timescale limit of albite decomposition during impact loading. These results refine interpretations of shock metamorphism in plagioclase under planetary impact conditions.

Plain Language Summary Meteorite impacts generate intense shock waves that create extremely high pressures and temperatures, rapidly altering the structure of minerals. Plagioclase, one of the most common minerals in planetary crusts, often preserves these shock features and provides important clues to the history of impact events. In this study, we compressed albite, a sodium-rich plagioclase, with laser-driven shock waves and directly tracked its crystal structure using the intense, ultrafast X-ray pulses. We observed that the crystal structure of albite collapsed into an amorphous, glass-like state during shock compression but returned to its original crystalline form once the shock was released. Other possible crystal structural changes were hindered because the shock conditions lasted only nanoseconds, demonstrating that the kinetics and duration of shock loading, rather than pressure alone, control mineral transformations during impacts.

1. Introduction

Plagioclase feldspars are the most abundant mineral group found on the surface of the Earth (Deer et al., 2001). They are also major constituents of meteorites (Jones, 2024), and high-pressure polymorphs and its related phases of plagioclase have been identified in shocked meteorites (e.g., Agarwal et al., 2016; Baziotis et al., 2013; Miyahara et al., 2017; Ozawa et al., 2014). Therefore, the high-pressure and temperature (high *P-T*) behavior of plagioclase has been of great interest for studies of meteorite impacts and crustal processes, as extreme conditions could induce crystal structure changes (Downs et al., 1994; Kubo et al., 2010; Tomioka et al., 2010; Tribaudino et al., 2011).

For the sodium end-member, albite (ideally $NaAlSi_3O_8$), high *P-T* forms as a product of impact events have been reported in natural rocks, including the amorphous state, the high-pressure crystalline polymorph (lingunite), and a decomposed form (jadeite + SiO_2) (Tomioka & Miyahara, 2017). The amorphous state of plagioclase can form

Visualization: Sota Takagi
Writing – original draft: Sota Takagi
Writing – review & editing: Sota Takagi, Naoko Takahashi, Hiroki Kobayashi, Donghoon Kim

either through solid-state amorphization or by shock-induced melting followed by rapid quenching of a dense melt at high pressure. The former is characterized by the absence of melting, whereas the latter is distinguished by smooth surfaces indicative of melting and quenching in natural samples (Chen & El Goresy, 2000; El Goresy et al., 2013). Such amorphous states serve as potential barometers of the past shock conditions. The pressure range for albite amorphization, however, varies considerably among studies. Laboratory shock-recovery experiments reported the onset pressures of partial amorphization at ∼30 GPa (Johnson & Hörz, 2003; Velde et al., 1989) or ∼50–56 GPa (Jaret et al., 2018), and complete amorphization at ∼35 GPa (Johnson & Hörz, 2003) or above 56 GPa (Jaret et al., 2018; Velde et al., 1989). Although the shock metamorphic classifications of Stöffler et al. (2018) assigned diaplectic glass and melting of albitic plagioclase to 34–45 GPa and >45 GPa, respectively, the wide scatter in experimental results highlights the need for further constraints on the mechanisms and conditions of albite (Na end-member) amorphization.

Decomposition of albite into jadeite ($NaAlSi_2O_6$) and SiO_2 under high *P-T* conditions is also a well-known phenomenon in static experiments. Jadeite is one of the most common high-pressure minerals in meteorites and has been interpreted to form either by solid-state transformation of albitic-plagioclase or by crystallization from melt (Ohtani et al., 2017). However, despite its common occurrence in natural shocked rocks, jadeite has not been reproduced in laboratory shock recovery experiments. Static high *P-T* studies demonstrated that the decomposition of amorphous albite into jadeite + SiO_2, as well as further transformation into Ca-ferrite-type $NaAlSiO_4$ + stishovite at higher pressures, requires elevated temperatures and longer timescales ($>10^2$ s), indicating that these processes are kinetically-controlled (Kubo et al., 2010). Although results imply that short-duration shock events may suppress decomposition reactions, direct experimental constraints on the behavior of albite under shock compression timescales remain scarce. As a result, the role of kinetics in controlling phase decomposition during impact-induced shock compression is still poorly understood.

Experimental data for albite under dynamic compression have been primarily obtained from Hugoniot measurements, in which the equation of state was determined from macroscopic velocity data. For albite-rich rock (albitite), Hugoniot data cover a range of approximately 13–90 GPa (Marsh, 1980; McQueen et al., 1967). Similar to other plagioclase minerals, the Hugoniot of albitite shows a distinct kink at ∼30–40 GPa in the pressure–density relation. The feature has been interpreted as reflecting a pressure-induced phase transition to a high-pressure structure, potentially of hollandite-type phase (Sekine & Ahrens, 1992). However, such a phase has not been identified in laboratory shock recovered samples (Jaret et al., 2018; Johnson et al., 2003; Johnson & Hörz, 2003; Velde et al., 1989), leaving the microscopic nature of the phase transition along the Hugoniot unresolved.

While dynamic diamond anvil cell experiments allow access to timescales longer than those of shock experiments and approaching those of meteorite impacts, reproducing the shock-compression pathway characteristic of natural impacts remains challenging. Laser-driven shock compression uniquely accesses high-*PT* states along the Hugoniot and enables in situ observation of crystal structure evolution under shock-loading conditions. To directly clarify the phase dynamics and kinetics of albite around ∼30–40 GPa under shock compression, we therefore conducted in situ X-ray diffraction (XRD) measurements during laser-driven shock compression, allowing direct tracking of structural response along the Hugoniot.

2. Materials and Methods

Natural albite crystals from New Idria, California, were used in this study. No impurity phase was detected in the powder XRD pattern (Figure S1 in Supporting Information S1). The presence of diffraction peaks inconsistent with high-albite (e.g., $\bar{1}32$ and $24\bar{1}$) (Winter et al., 1979) indicated that the sample predominantly consisted of low-albite. The chemical composition, determined by electron probe microanalyzer (EPMA), confirms that the sample was highly pure albite (Ab_{100}) (Table S1 in Supporting Information S1). In order to prepare polycrystalline samples, the albite samples were crushed by an agate mortar and then sintered at 1100°C and 50 MPa for 5 min using a Spark Plasma Sintering (SPS) apparatus (Fuji Electronic Industrial, Japan). The apparent density of the sintered albite was 2.59(3) g/cm^3, measured by Archimedes' method, corresponding to 99.1% of the crystal density (2.61 g/cm^3). The sintered material retained the crystal structure of low-albite. Qualitative energy-dispersive X-ray spectroscopic (EDS) area analysis confirmed that the chemical composition remained unchanged before and after the sintering, although minor heterogeneity was observed in micrometer scale (Table S2 and Figure S2 in Supporting Information S1). The sintered samples were cut and polished to ∼2 × 2 mm^2 square with a thickness of ∼35 μm. A ∼25-μm-thick black Kapton was glued to the sample surface as a laser ablator.

10.1029/2025GL119542

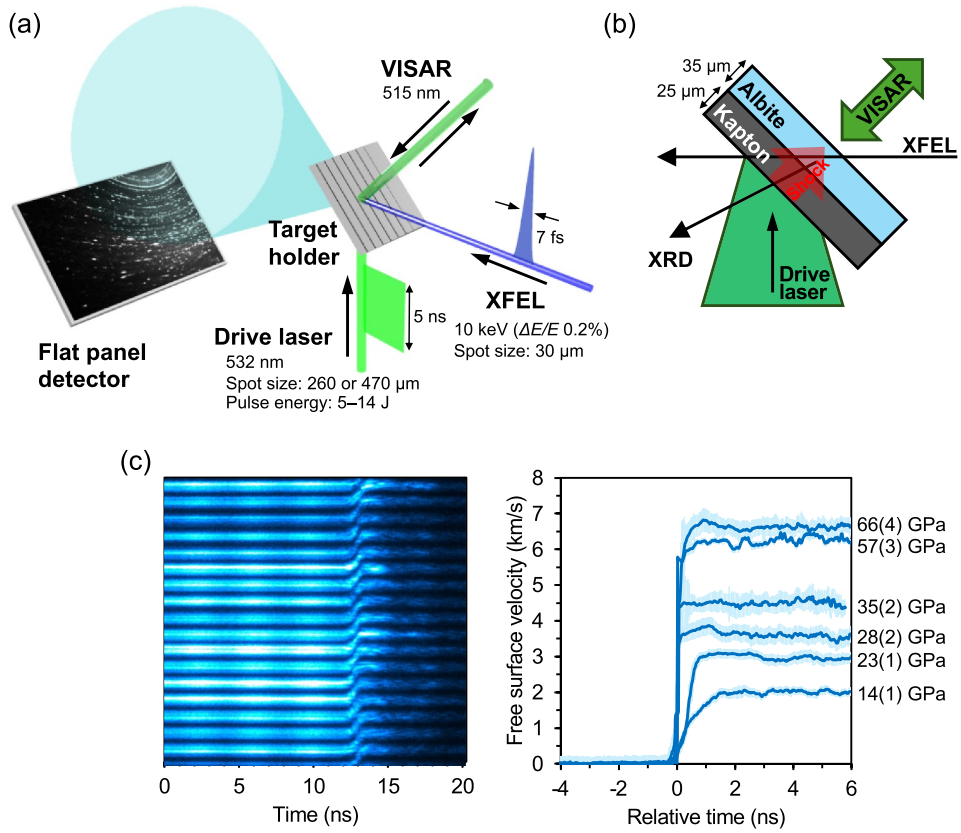

Figure 1. (a) Experimental configuration of the laser-shock in situ XRD experiments, and (b) configuration around the target. (c) Representative VISAR image for run #1477848 with velocity-per-fringe of 2.894 km/s and free surface velocity histories in relative time around the shock breakout timing of six different conditions. Using the peak value of the free surface velocity (u_{fs}) and the error, particle velocity (u_p) was calculated with the free surface approximation of $u_p = u_{fs}/2$ (Forbes, 2012). The peak shock pressure, P (GPa), was estimated with initial density, ρ_0 (g/cm^3), and shock wave velocity, U_s (km/s), by $P = \rho_0 U_s u_p$.

Laser-driven shock compression experiments were conducted at the Experimental Hutch 5 (EH5) on the Beamline 3 (BL3) at the SPring-8 Angstrom Compact Free-Electron Laser (SACLA) facility (Inubushi et al., 2020). Figure 1a shows the experimental configuration. A single shock wave was generated by one laser pulse, and in situ XRD and velocity data were obtained using synchronized X-ray and optical laser pulses. As the laser irradiation caused a severe damage on the target, it was replaced with a fresh one, and the measurements were repeated under different shot conditions. The incident angle between the drive laser and X-ray was about 90°, and the target plates were tilted at 45° to the drive laser (Figure 1b).

A high-power nanosecond laser (Hamamatsu Photonics, Japan) with a wavelength of 532 nm and a ∼5-ns quasi-square pulse was used to generate shock waves. A quasi-flat-top spatial profile of ∼260 or ∼470 μm (FWHM) on the target was achieved using a phase plate. Laser pulse energy was adjusted to values between ∼3 and 14 J/pulse using attenuators. The relative timing between the drive laser and X-ray pulses was controlled by an electrical delay system with a timing jitter <30 ps (root mean square). A quasi-monochromatic X-ray pulse with an energy of 10.01(1) keV (or 10.004(8) keV for Run #1564530), a bandwidth of $\Delta E/E$ ∼0.2%, and a duration of ∼7 fs was used as the probe. The X-ray beam was focused to ∼20 μm (vertical) and ∼30 μm (horizontal) at the target using KB mirrors. A single X-ray pulse from a 30 Hz repetition was isolated by a pulse selector to obtain an ultrafast snapshot. Two-dimensional (2D) XRD images were recorded on a flat-panel detector (204 × 153 mm^2, pixel size 99 × 99 μm) (Rad-icon 1520, Teledyne DALSA). This geometry provided XRD coverage over scattering angles (2θ) of ∼15–80° and azimuth angles of ∼0–100° in transmission. Calibration was performed using diffraction images of polycrystalline CeO_2 (NIST SRM 674b). One-dimensional (1D) integration of XRD was performed

Table 1
Experimental Parameters for the Data at Compression Conditions, Phase From XRD, and Peak Positions of FSDP and SSDP (Q1 and Q2)

Run number	Laser energy (J)	Laser spot size (μm)	Peak pressure (GPa)	Density (g/cm^3)	X-ray probe time relative to breakout (ns)	Phase	Q1 (Å^{-1})	Q2 (Å^{-1})
1477570	13.3	260	66(4)	4.58(51)	+0.4	Amorphous	2.43	3.06
1564530	8.4	260	57(3)	4.48(40)	+0.3	Amorphous	2.52	3.14
1477643	6.8	260	35(2)	4.13(28)	−0.2	Amorphous	2.41	3.11
1477584	5.0	260	28(2)	3.80(21)	−0.3	Amorphous	2.32	3.04
1477848	12.5	470	23(1)	3.53(12)	−0.2	Compressed ab + Amorphous	2.19	3.02
1477858	5.7	470	14(1)	3.15(6)	−1.1	Ambient ab + Compressed ab	–	–

Note. Pressure and density are estimated with VISAR data and the Rankine-Hugoniot equation.

using the pyFAI package (Kieffer et al., 2020). The XRD probe timings relative to breakout timing are summarized in Table 1.

Free surface velocities of the sample rear surface were measured using a line-imaging velocity interferometer system for any reflector (VISAR) (Celliers et al., 2004). The VISAR had a field of view of ∼300 μm and a sweep duration of ∼20 ns (Figure 1c). Fringe shifts were analyzed using Neutrino software (Copyright 2013; Alessandro Flacco, Tommaso Vinci). The free surface velocity histories are summarized in Figure 1c. Using fitted parameters of the albitite U_s–u_p relation (U_s = 5.19(15) + 0.36(6)u_p for u_p < ∼2.4 km/s, U_s = 2.42(11) + 1.58(3)u_p for u_p > ∼2.4 km/s) (Marsh, 1980; McQueen et al., 1967), the peak pressures for the six shots were estimated to be 14 (1), 23(1), 28(2), 35(2), 57(3), and 66(4) GPa (Table 1). Throughout the manuscript, pressures derived from VISAR measurements are used.

3. Results

Figure 2 shows the in situ XRD patterns at compressed timing. At 14 GPa, diffraction peaks of compressed albite appeared at smaller *d*-spacing of the peaks of ambient albite. The shifted peaks can be assigned to compressed albite with a density of 2.90 g/cm^3 (Figure S3 in Supporting Information S1). The density derived from XRD is slightly lower than that from VISAR (3.15 g/cm^3), likely reflecting a pressure gradient within the sample caused by rarefaction waves propagating from the laser-irradiated surface (Figure S4 in Supporting Information S1). At 23 GPa, two broad diffuse features appeared at *d*-spacings of ∼2.8 Å and ∼2.1 Å, indicating the amorphization of albite. Minor crystalline peaks can be attributed to compressed albite. The VISAR density at this condition is 3.53 (12) g/cm^3. Simulated XRD patterns of jadeite, lingunite, and Ca-ferrite-type $NaAlSiO_4$ do not match the observed pattern (Figure S3 in Supporting Information S1). The XRD density of compressed albite was calculated to be 3.58(5) g/cm^3, consistent with the VISAR density. Above 28 GPa and up to 66 GPa, the diffraction patterns are dominated by broad diffuse features with only minor contributions from uncompressed or released albite, indicating a complete amorphization under compression. No diffraction peaks corresponding to jadeite or Ca-ferrite-type $NaAlSiO_4$ were observed during compression.

Figure 3 shows the time evolution of the XRD patterns in the 28, 35, and 66-GPa shots. At all conditions, the peak positions of the diffuse features shifted to larger *d*-spacings, and sharp diffraction peaks appeared with time. The position of the crystalline peaks overlapped with the original peaks at ambient conditions, indicating recovery of crystalline albite. Crystalline signals appeared within ∼11 and ∼31 ns after shock breakout in the 28-GPa and 35-GPa shots, respectively. In the 66-GPa shots, crystalline signals were not detected at 32 ns after shock breakout, but it emerged only at later time (>91 ns).

The shock compression conditions of the present study are plotted on a pressure-temperature (*P*-*T*) diagram together with reported phase relations of albite from static high *P*-*T* experiments (Figure 4a). Shock temperatures along the Hugoniot were calculated using the Mie-Grüneisen-Debye model. The thermodynamic parameters of albite used in these calculations are summarized in Table S4 of Supporting Information S1. Pressure and density derived from VISAR are plotted in Figure 4b together with previous Hugoniot data. The in situ XRD data show amorphization across the investigated pressure range, including conditions beyond equilibrium phase boundaries inferred from static experiments.

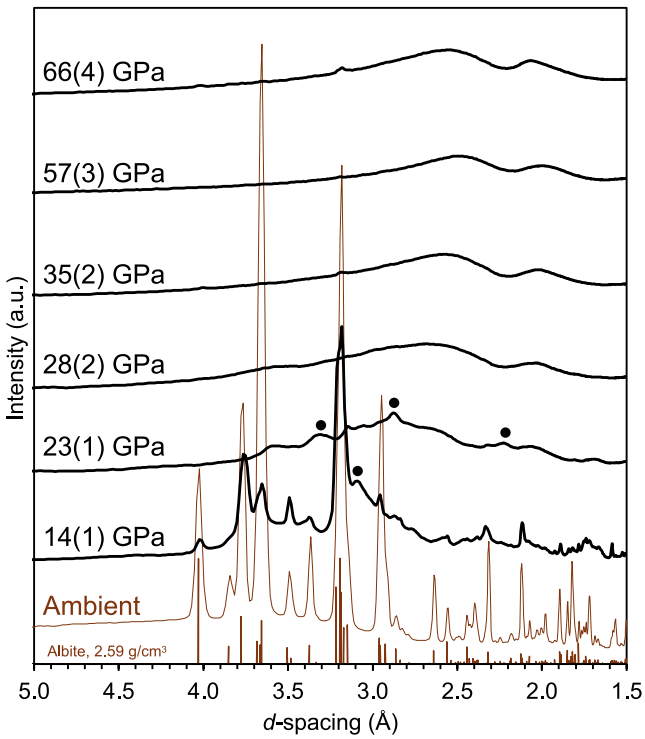

Figure 2. Pressure-dependent in situ XRD patterns for albite. A simulated pattern of albite using the crystallographic information file (Harlow & Brown, 1980) in American Mineralogist Crystal Structure Database is shown as brown line. Representative peaks of compressed albite are marked with black dots.

4. Discussion

Although decomposition of albite into jadeite + SiO_2 or Ca-ferrite-type $NaAlSiO_4$ + SiO_2 is thermodynamically favored under high *P-T* conditions, our in situ XRD results demonstrate that such reactions are kinetically inhibited under nanosecond shock compression. No crystalline decomposition products were observed, despite shock paths traversing *P-T* conditions where these phases are predicted to be stable. Static high *P-T* experiments indicate that decomposition of amorphous albite requires elevated temperatures and long timescales ($\sim 10^2$ s), highlighting strong kinetic control (Kubo et al., 2010). Phase relations for plagioclase (labradorite (An_{51}) and anorthite (An_{96})) reported by Xie et al. (2025) further indicate that decomposition is thermodynamically favored at *P-T* conditions comparable to those reached in the 57-GPa shot. Nevertheless, no jadeite or Ca-ferrite-type phases were detected, indicating that nanosecond shock durations and extreme strain rates ($\sim 10^8$ s^{-1}) are insufficient to overcome the kinetic barriers required for nucleation and growth. Previous laser-driven shock experiments on plagioclase (labradorite (An_{53})) up to ~30 GPa similarly reported amorphization without decomposition (Gleason et al., 2022). By extending the pressure range to 66 GPa, our results demonstrate that kinetic suppression of albite decomposition persists across a wide range of shock-accessible conditions. Similar suppression of reconstructive and decompression reactions that require significant atomic rearrangement has been reported for other silicates under nanosecond shock compression, suggesting that this behavior is a general kinetic limitation (Kim et al., 2021; Takagi et al., 2022).

Our in situ XRD results resolved the long-standing ambiguity regarding the origin of the kink in the albite Hugoniot at ~30–40 GPa, demonstrating that high-pressure regime is dominated by amorphization rather than by transformation to a hollandite-type phase as proposed by Sekine and Ahrens (1992) or an equilibrium Ca-ferrite-type phase (Figure 4b).

Under nanosecond shock compression, albite predominantly undergoes amorphization rather than transformation into crystalline high-pressure phases. The in situ XRD patterns are characterized by broad diffuse features, consistent with recent shock studies on silicate glasses and shock-amorphized silicates, which show that materials

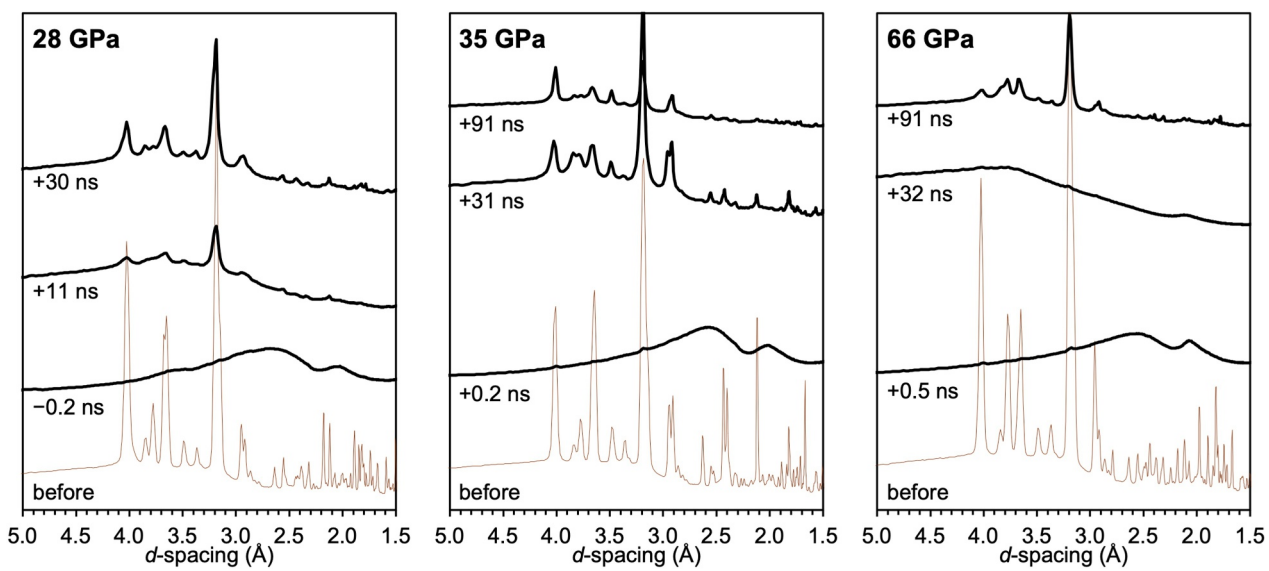

Figure 3. Time evolution of in situ XRD patterns. X-ray delay timing compared with the shock breakout is displayed with XRD pattern.

10.1029/2025GL119542

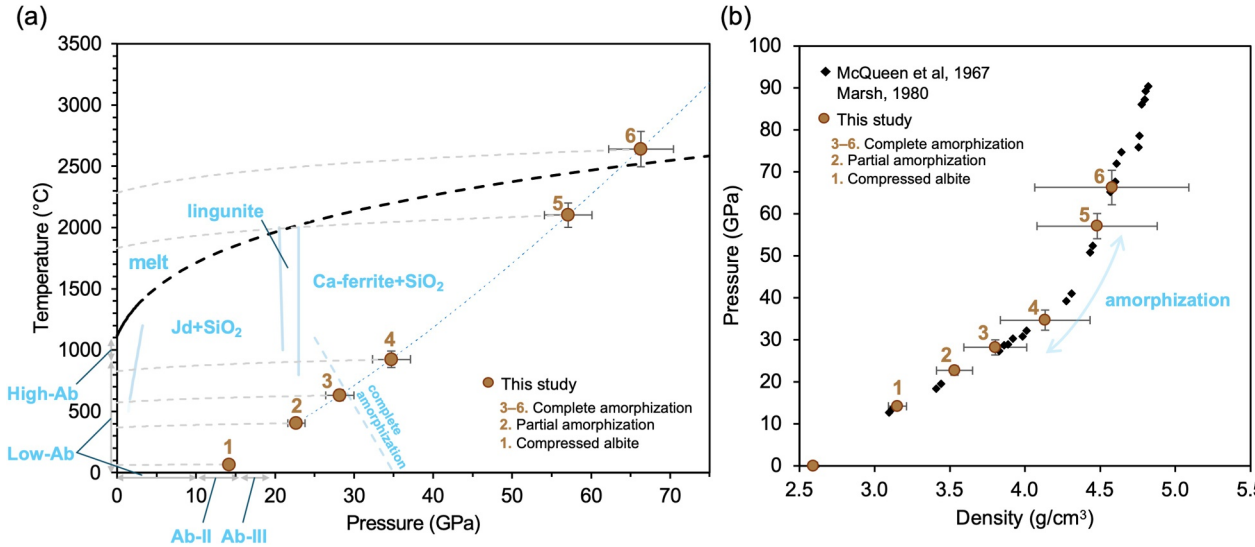

Figure 4. (a) Pressure-temperature conditions of the six shock compression data. The release isentrope curves from each compression condition are shown as dotted gray lines. The melting curve is drawn with the previous data up to ~3.2 GPa (Boyd & England, 1963) and the extrapolation with the Simon equation, P (GPa) = 1.95[(T (K)/1391)$^{5.1}$ − 1]. The phase changes reported in static high P-T experiments are shown with light blue line and letters. The references are as follows; High/low albite boundary (Winter et al., 1979), melting curve (Boyd & England, 1963), ab-II and ab-III (Pakhomova et al., 2020), Jd + SiO_2 (Birch & Lecomte, 1960; Holland, 1980; Johannes et al., 1971; Newton & Smith, 1967), hollandite-type phase (Liu, 1978; Tutti, 2007), complete amorphization lines (Kubo et al., 2010; Sims et al., 2020; Tomioka et al., 2010), and Ca-ferrite + SiO_2 (Liu, 1978; Yagi et al., 1994). (b) Hugoniot density-pressure relation of albite. The pressure and density of the present study are determined by VISAR measurements and Hugoniot parameter in the previous studies (Marsh, 1980; McQueen et al., 1967).

tend to be amorphized under nanosecond timescales rather than stabilize as crystalline phases (Crépisson et al., 2025; Feng et al., 2025; Hernandez et al., 2020; Kim et al., 2021; Umeda et al., 2025). Despite the limited Q range, structural evolution during compression and release can be inferred from diffuse scattering features (Figure 2). The positions of the first and second sharp diffraction peaks (FSDP and SSDP) shift to lower d-spacing with increasing pressure (Table 1). These peak positions were extracted directly from the scattering intensity profiles, as reliable background subtraction was not feasible. These shifts are consistent with densification trends reported for albite glass under static compression (Sakamaki et al., 2014). The FSDP shift reflects shrinkage of intermediate-range order, whereas the SSDP shift is linked to increased cation–anion coordination and network densification (Morard et al., 2020; Sakamaki et al., 2014). Consequently, our XRD data suggest that amorphized albite densifies along the Hugoniot accompanied by an increase of coordination number. The 66-GPa data point deviates from the overall trend, likely because the X-ray probe timing was after the onset of pressure release. During release, the FSDP shifts to larger d-spacing and the SSDP disappears, indicating volume expansion and reduced coordination, consistent with a decrease in coordination number and leading to back transformation into crystalline albite.

To interpret the appearance of crystalline diffraction peaks during pressure release, post-shock temperatures were estimated along release isentropes. Release paths were calculated by assuming isentropic decompression from peak Hugoniot states using the Mie-Grüneisen-Debye model. As shown in Figure 4a, the release isentropes for the 35-GPa and lower-pressure shots remain below the melting curve of albite, indicating that these samples did not experience melting during shock compression or release. Thus, recovery of crystalline diffraction peaks in these shots is unlikely to reflect recrystallization from melt. Instead, this behavior is consistent with reversible amorphization reported for plagioclase in diamond anvil cell experiments (Sims et al., 2020) and laser-driven shock experiments (Gleason et al., 2022), in which crystalline order is temporarily disrupted under compression but recovers upon decompression. In contrast, the post-shock temperatures estimated for the 57- and 66-GPa shots exceed the melting temperature of albite, suggesting that melting may occur under these conditions (Figure 4a). The delayed appearance of crystalline peaks in the 66-GPa shot is consistent with crystallization from a transient melt during release (Figure 3). However, diffraction peak widths and intensities show no systematic differences among the shots, preventing a clear distinction between solid-state recovery of crystalline state and recrystallization from melt based on the present XRD data. Additional constraints will be required to discriminate between these mechanisms.

The present results provide a framework for understanding the wide scatter in reported amorphization pressures of plagioclase in laboratory shock-recovery experiments. Previous shock recovery studies report partial to complete amorphization over a broad pressure range (~30 to >55 GPa) (e.g., Jaret et al., 2018; Johnson & Hörz, 2003; Velde et al., 1989). Our in situ XRD data show that shock-induced amorphization can be transient, with structural recovery during release depending sensitively on pressure–temperature–time conditions. Thus, the recovered state may reflect the integrated pressure–temperature–time history rather than peak pressure alone, providing a natural explanation for the variability reported in shock-recovery experiments.

With respect to natural impacts, the duration of shock loading is generally longer than in laser-driven shock experiments, and post-shock temperatures are often higher due to larger spatial scales and sustained energy deposition. Under such conditions, kinetic barriers to decomposition may be partially overcome, allowing formation of jadeite or related high-pressure phases in natural shocked rocks. In this context, the occurrence of jadeite in natural shocked rocks can serve as a valuable constraint on the pressure–temperature–time conditions of impact events, reflecting not only peak pressure but also the duration of high-temperature conditions, as indicated by kinetic studies of albite decomposition (Kubo et al., 2010; Ohtani et al., 2017). At present, kinetic constraints relevant to impact processes are largely inferred from static high-pressure experiments, whereas direct experimental constraints on mineral behavior under extremely short shock-compression timescales remain limited. Although the nanosecond duration of laser-driven shock experiments is shorter than that of natural impacts, these experiments define the short-timescale limit of phase transformations, where kinetic suppression dominates even at pressures exceeding equilibrium phase boundaries. Together with static high-pressure experiments that constrain long-timescale kinetics, laser-driven shock experiments provide essential bounds on the pressure–temperature–time conditions governing phase transformations in plagioclase during impact events. Future studies at intermediate timescales, such as dynamic diamond anvil cell experiments, will be crucial to further bridge laboratory shock experiments and natural impact conditions.

5. Conclusions

Shock compression dynamics of albite were investigated by in situ X-ray diffraction. Albite maintained its crystal structure up to 14 GPa and transformed into an amorphous state above 28 GPa. No evidence for the formation of lingunite, jadeite, or Ca-ferrite-type $NaAlSiO_4$ was observed during compression or release. These results demonstrate that the high-pressure region of the albite Hugoniot is dominated by amorphization rather than by crystalline high-pressure phases, resolving the long-standing ambiguity in its shock response. Amorphization was accompanied by densification and an increase in coordination number. Upon pressure release, the amorphous structure expanded and the crystalline structure was recovered, reflecting reversible amorphization and/or recrystallization promoted by elevated temperatures and short timescale. The absence of decomposition products indicates that albite decomposition is kinetically inhibited at nanosecond timescales, even at pressures exceeding equilibrium phase boundaries. These results define the short-timescale limit of phase transformations in albite and highlight the critical role of kinetics and duration of high *P-T* states in shock-induced mineral transformations relevant to planetary impact processes.

Conflict of Interest

The authors declare no conflicts of interest relevant to this study.

Availability Statement

Datasets for this study have been deposited in Zenodo (Takagi, 2025).

Acknowledgments

This work was supported by the Japan Society for the Promotion of Science (JSPS) KAKENHI (Grant 21J01027, 22K14128, 24K17142, 23K20038, and 25H00618), MEXT QLEAP program (JPMXS0118067246), Grants from the National Research Foundation (NRF) of Korea funded by the Ministry of Science and ICT (RS-2023-00284250 and RS-2024-00342193), Global - Learning & Academic research institution for Master's PhD students, and Postdocs (LAMP) Program of NRF Grant funded by the Ministry of Education (RS-2023-00301938), and from a Korea University Grant. The experiments were performed at the BL3 of SACLA with the approval of the Japan Synchrotron Radiation Research Institute (JASRI) (Proposal 2022A8064, 2024B8012, and 2025A8027). The experimental results were obtained using a high-power nanosecond laser deployed at SACLA by Institute of Laser Engineering of Osaka University. This work was also supported by the Joint Usage/Research Center PRIUS, Ehime University, Japan. We appreciate Prof. Tatsuki Tsujimori from Tohoku University for supplying natural albite samples. We also appreciate Gunhee Lee, Mujin Lee, Jeonguk Park, and Junghun Kim from Korea University for their supports in experiments at SACLA.

References

Agarwal, A., Reznik, B., Kontny, A., Heissler, S., & Schilling, F. (2016). Lingunite-a high-pressure plagioclase polymorph at mineral interfaces in doleritic rock of the Lockne impact structure (Sweden). *Scientific Reports*, *6*(1), 25991. https://doi.org/10.1038/srep25991

Baziotis, I. P., Liu, Y., DeCarli, P. S., Melosh, H. J., McSween, H. Y., Bodnar, R. J., & Taylor, L. A. (2013). The Tissint Martian meteorite as evidence for the largest impact excavation. *Nature Communications*, *4*(1), 1404. https://doi.org/10.1038/ncomms2414

Birch, A. F., & Lecomte, P. (1960). Temperature-pressure plane for albite composition. *American Journal of Science*, *258*(3), 209–217. https://doi.org/10.2475/ajs.258.3.209

Boyd, F. R., & England, J. L. (1963). Effect of pressure on the melting of diopside, $CaMgSi_2O_6$, and albite, $NaAlSi_3O_8$, in the range up to 50 kilobars. *Journal of Geophysical Research (1896-1977)*, *68*(1), 311–323. https://doi.org/10.1029/JZ068i001p00311

Celliers, P. M., Bradley, D. K., Collins, G. W., Hicks, D. G., Boehly, T. R., & Armstrong, W. J. (2004). Line-imaging velocimeter for shock diagnostics at the OMEGA laser facility. *Review of Scientific Instruments*, *75*(11), 4916–4929. https://doi.org/10.1063/1.1807008

Chen, M., & El Goresy, A. (2000). The nature of maskelynite in shocked meteorites: Not diaplectic glass but a glass quenched from shock-induced dense melt at high pressures. *Earth and Planetary Science Letters*, *179*(3), 489–502. https://doi.org/10.1016/S0012-821X(00)00130-8

Crépisson, C., Amouretti, A., Harmand, M., Sanloup, C., Heighway, P., Azadi, S., et al. (2025). Shock-driven amorphization and melting in Fe_2O_3. *Physical Review B*, *111*(2), 024209. https://doi.org/10.1103/PhysRevB.111.024209

Deer, W. A., Howie, R. A., & Zussman, J. (2001). Rock-forming minerals. *Geological Society of London*.

Downs, R. T., Hazen, R. M., & Finger, L. W. (1994). The high-pressure crystal chemistry of low albite and the origin of the pressure dependency of Al-Si ordering. *American Mineralogist*, *79*(11–12), 1042–1052.

El Goresy, A., Gillet, P., Miyahara, M., Ohtani, E., Ozawa, S., Beck, P., & Montagnac, G. (2013). Shock-induced deformation of Shergottites: Shock-pressures and perturbations of magmatic ages on Mars. *Geochimica et Cosmochimica Acta*, *101*, 233–262. https://doi.org/10.1016/j.gca.2012.10.002

Feng, X., Pan, S., Katagiri, K., Shi, J., Qu, J., Nonaka, K., et al. (2025). Nanosecond structural evolution in shocked coesite. *Science Advances*, *11*(17), eads3139. https://doi.org/10.1126/sciadv.ads3139

Forbes, J. W. (2012). *Shock wave compression of condensed matter*. A Primer.

Gleason, A. E., Park, S., Rittman, D. R., Ravasio, A., Langenhorst, F., Bolis, R. M., et al. (2022). Ultrafast structural response of shock-compressed plagioclase. *Meteoritics & Planetary Science*, *57*(3), 635–643. https://doi.org/10.1111/maps.13785

Harlow, G. E., & Brown, G. E. (1980). Low albite: An X-ray and neutron diffraction study. *American Mineralogist*, *65*(9–10), 986–995.

Hernandez, J. A., Morard, G., Guarguaglini, M., Alonso-Mori, R., Benuzzi-Mounaix, A., Bolis, R., et al. (2020). Direct observation of shock-induced disordering of enstatite below the melting temperature. *Geophysical Research Letters*, *47*(15), e2020GL088887. https://doi.org/10.1029/2020gl088887

Holland, T. J. B. (1980). The reaction albite = jadeite+quartz determined experimentally in the range 600°C–1200°C. *American Mineralogist*, *65*(1–2), 129–134.

Inubushi, Y., Yabuuchi, T., Togashi, T., Sueda, K., Miyanishi, K., Tange, Y., et al. (2020). Development of an experimental platform for combinative use of an XFEL and a high-power nanosecond laser. *Applied Sciences*, *10*(7), 2224. https://doi.org/10.3390/app10072224

Jaret, S. J., Johnson, J. R., Sims, M., DiFrancesco, N., & Glotch, T. D. (2018). Microspectroscopic and petrographic comparison of experimentally shocked Albite, andesine, and bytownite. *Journal of Geophysical Research: Planets*, *123*(7), 1701–1722. https://doi.org/10.1029/2018je005523

Johannes, W., Bell, P. M., Mao, H. K., Boettcher, A. L., Chipman, D. W., Hays, J. F., et al. (1971). An interlaboratory comparison of piston-cylinder pressure calibration using the albite-breakdown reaction. *Contributions to Mineralogy and Petrology*, *32*(1), 24–38. https://doi.org/10.1007/BF00372231

Johnson, J. R., & Hörz, F. (2003). Visible/near-infrared spectra of experimentally shocked plagioclase feldspars. *Journal of Geophysical Research*, *108*(E11). https://doi.org/10.1029/2003JE002127

Johnson, J. R., Horz, F., & Staid, M. I. (2003). Thermal infrared spectroscopy and modeling of experimentally shocked plagioclase feldspars. *American Mineralogist*, *88*(10), 1575–1582. https://doi.org/10.2138/am-2003-1020

Jones, R. H. (2024). Meteorites and planet formation. *Reviews in Mineralogy and Geochemistry*, *90*(1), 113–140. https://doi.org/10.2138/rmg.2024.90.04

Kieffer, J., Valls, V., Blanc, N., & Hennig, C. (2020). New tools for calibrating diffraction setups. *Journal of Synchrotron Radiation*, *27*(2), 558–566. https://doi.org/10.1107/s1600577520000776

Kim, D., Tracy, S. J., Smith, R. F., Gleason, A. E., Bolme, C. A., Prakapenka, V. B., et al. (2021). Femtosecond X-ray diffraction of laser-shocked Forsterite (Mg_2SiO_4) to 122 GPa. *Journal of Geophysical Research: Solid Earth*, *126*(1), e2020JB020337. https://doi.org/10.1029/2020jb020337

Kubo, T., Kimura, M., Kato, T., Nishi, M., Tominaga, A., Kikegawa, T., & Funakoshi, K.-i. (2010). Plagioclase breakdown as an indicator for shock conditions of meteorites. *Nature Geoscience*, *3*(1), 41–45. https://doi.org/10.1038/ngeo704

Liu, L.-G. (1978). High-pressure phase transformations of albite, jadeite and nepheline. *Earth and Planetary Science Letters*, *37*(3), 438–444. https://doi.org/10.1016/0012-821x(78)90059-6

Marsh, S. P. (1980). *LASL shock Hugoniot data*. University of California Press.

McQueen, R. G., Marsh, S. P., & Fritz, J. N. (1967). Hugoniot equation of state of twelve rocks. *Journal of Geophysical Research (1896-1977)*, *72*(20), 4999–5036. https://doi.org/10.1029/JZ072i020p04999

Miyahara, M., Ohtani, E., & Yamaguchi, A. (2017). Albite dissociation reaction in the Northwest Africa 8275 shocked LL chondrite and implications for its impact history. *Geochimica et Cosmochimica Acta*, *217*, 320–333. https://doi.org/10.1016/j.gca.2017.08.034

Morard, G., Hernandez, J. A., Guarguaglini, M., Bolis, R., Benuzzi-Mounaix, A., Vinci, T., et al. (2020). In situ X-ray diffraction of silicate liquids and glasses under dynamic and static compression to megabar pressures. *Proceedings of the National Academy of Sciences*, *117*(22), 11981–11986. https://doi.org/10.1073/pnas.1920470117

Newton, R. C., & Smith, J. V. (1967). Investigations concerning the breakdown of Albite at depth in the Earth. *The Journal of Geology*, *75*(3), 268–286. https://doi.org/10.1086/627255

Ohtani, E., Ozawa, S., & Miyahara, M. (2017). Jadeite in shocked meteorites and its textural variations. *Journal of Mineralogical and Petrological Sciences*, *112*(5), 247–255. https://doi.org/10.2465/jmps.170329

Ozawa, S., Miyahara, M., Ohtani, E., Koroleva, O. N., Ito, Y., Litasov, K. D., & Pokhilenko, N. P. (2014). Jadeite in Chelyabinsk meteorite and the nature of an impact event on its parent body. *Scientific Reports*, *4*(1), 5033. https://doi.org/10.1038/srep05033

Pakhomova, A., Simonova, D., Koemets, I., Koemets, E., Aprilis, G., Bykov, M., et al. (2020). Polymorphism of feldspars above 10 GPa. *Nature Communications*, *11*(1), 2721. https://doi.org/10.1038/s41467-020-16547-4

Sakamaki, T., Kono, Y., Wang, Y., Park, C., Yu, T., Jing, Z., & Shen, G. (2014). Contrasting sound velocity and intermediate-range structural order between polymerized and depolymerized silicate glasses under pressure. *Earth and Planetary Science Letters*, *391*, 288–295. https://doi.org/10.1016/j.epsl.2014.02.008

Sekine, T., & Ahrens, T. J. (1992). Shock-induced transformations in the system $NaAlSiO_4$—SiO_2: A new interpretation. *Physics and Chemistry of Minerals*, *18*(6), 359–364. https://doi.org/10.1007/BF00199416

Sims, M., Jaret, S. J., Johnson, J. R., Whitaker, M. L., & Glotch, T. D. (2020). Unconventional high-pressure Raman spectroscopy study of kinetic and peak pressure effects in plagioclase feldspars. *Physics and Chemistry of Minerals*, *47*(2), 12. https://doi.org/10.1007/s00269-020-01080-z

Stöffler, D., Hamann, C., & Metzler, K. (2018). Shock metamorphism of planetary silicate rocks and sediments: Proposal for an updated classification system. *Meteoritics & Planetary Science*, *53*(1), 5–49. https://doi.org/10.1111/maps.12912

Takagi, S. (2025). Dataset for laser-shock experiments for albite at SACLA (2024B and 2025A) [Dataset]. *Zenodo*. https://doi.org/10.5281/zenodo.17148873

Takagi, S., Ichiyanagi, K., Kyono, A., Kawai, N., Nozawa, S., Ozaki, N., et al. (2022). Phase transition and melting in zircon by nanosecond shock loading. *Physics and Chemistry of Minerals*, *49*(5), 8. https://doi.org/10.1007/s00269-022-01184-8

Tomioka, N., Kondo, H., Kunikata, A., & Nagai, T. (2010). Pressure-induced amorphization of albitic plagioclase in an externally heated diamond anvil cell. *Geophysical Research Letters*, *37*(21). https://doi.org/10.1029/2010GL044221

Tomioka, N., & Miyahara, M. (2017). High-pressure minerals in shocked meteorites. *Meteoritics & Planetary Science*, *52*(9), 2017–2039. https://doi.org/10.1111/maps.12902

Tribaudino, M., Bruno, M., Nestola, F., Pasqual, D., & Angel, R. J. (2011). Thermoelastic and thermodynamic properties of plagioclase feldspars from thermal expansion measurements. *American Mineralogist*, *96*(7), 992–1002. https://doi.org/10.2138/am.2011.3722

Tutti, F. (2007). Formation of end-member $NaAlSi_3O_8$ hollandite-type structure (lingunite) in diamond anvil cell. *Physics of the Earth and Planetary Interiors*, *161*(3–4), 143–149. https://doi.org/10.1016/j.pepi.2007.02.004

Umeda, Y., Ozaki, N., Sekine, T., Hironaka, Y., Inubushi, Y., Katagiri, K., et al. (2025). In situ observation of shock-induced structural evolution of calcite. *Physics and Chemistry of Minerals*, *52*(2), 20. https://doi.org/10.1007/s00269-025-01320-0

Velde, B., Syono, Y., Kikuchi, M., & Boyer, H. (1989). Raman microprobe study of synthetic diaplectic plagioclase feldspars. *Physics and Chemistry of Minerals*, *16*(5), 436–441. https://doi.org/10.1007/BF00197013

Winter, J. K., Okamura, F. P., & Ghose, S. (1979). A high-temperature structural study of high albite, monalbite, and the analbite-->monalbite phase transition. *American Mineralogist*, *64*, 409–423.

Xie, T., Shieh, S. R., Chariton, S., van Zyl, M., Rodriguez, R. D., Prakapenka, V. B., & Zhang, D. (2025). Plagioclase under compression: A path to diaplectic glass and maskelynite. *Science Advances*, *11*(25), eadv8231. https://doi.org/10.1126/sciadv.adv8231

Yagi, A., Suzuki, T., & Akaogi, M. (1994). High pressure transitions in the system $KAlSi_3O_8$-$NaAlSi_3O_8$. *Physics and Chemistry of Minerals*, *21*(1–2). https://doi.org/10.1007/bf00205210

References From the Supporting Information

Anselmi-Tamburini, U., Garay, J. E., & Munir, Z. A. (2005a). Fundamental investigations on the spark plasma sintering/synthesis process: III. Current effect on reactivity. *Materials Science and Engineering: A*, *407*(1), 24–30. https://doi.org/10.1016/j.msea.2005.06.066

Anselmi-Tamburini, U., Gennari, S., Garay, J. E., & Munir, Z. A. (2005b). Fundamental investigations on the spark plasma sintering/synthesis process: II. Modeling of current and temperature distributions. *Materials Science and Engineering: A*, *394*(1), 139–148. https://doi.org/10.1016/j.msea.2004.11.019

Chen, W., Anselmi-Tamburini, U., Garay, J. E., Groza, J. R., & Munir, Z. A. (2005). Fundamental investigations on the spark plasma sintering/synthesis process: I. Effect of dc pulsing on reactivity. *Materials Science and Engineering: A*, *394*(1), 132–138. https://doi.org/10.1016/j.msea.2004.11.020

Csáki, Š., Lukáč, F., Húlan, T., Veverka, J., & Knapek, M. (2021). Preparation of anorthite ceramics using SPS. *Journal of the European Ceramic Society*, *41*(8), 4618–4624. https://doi.org/10.1016/j.jeurceramsoc.2021.03.004

Hu, J., & Sharp, T. G. (2022). Formation, preservation and extinction of high-pressure minerals in meteorites: Temperature effects in shock metamorphism and shock classification. *Progress in Earth and Planetary Science*, *9*(1), 6. https://doi.org/10.1186/s40645-021-00463-2

Larsen, J. T., & Lane, S. M. (1994). HYADES—A plasma hydrodynamics code for dense plasma studies. *Journal of Quantitative Spectroscopy and Radiative Transfer*, *51*(1), 179–186. https://doi.org/10.1016/0022-4073(94)90078-7

Shigematsu, N., Zhou, Y., Hyuga, H., Yoshizawa, Y.-i., & Kido, M. (2022). Fabrication of dense albite aggregates by hot pressing. *Progress in Earth and Planetary Science*, *9*(1), 34. https://doi.org/10.1186/s40645-022-00492-5